

PDF hosted at the Radboud Repository of the Radboud University Nijmegen

The following full text is a publisher's version.

For additional information about this publication click this link.

<http://hdl.handle.net/2066/20659>

Please be advised that this information was generated on 2017-12-05 and may be subject to change.

Original Article

Monitoring Morphology and Signal During Non-radioactive In Situ Hybridization Procedures by Reflection-contrast Microscopy and Transmission Electron Microscopy¹

MERRYN V. E. MACVILLE,² ANNETTE G. M. VAN DORP, KARIEN C. WIESMEIJER, ROELAND W. DIRKS, JACK A. M. FRANSEN,³ and ANTON K. RAAP

Departments of Cytochemistry and Cytometry (MVEM,AGMD,KCW,RWD,AKR) and Electron Microscopy (MVEM,AGMD,KCW, JAMF), University of Leiden, Leiden, The Netherlands.

Received for publication August 16, 1994 and in revised form February 8, 1995; accepted February 16, 1995 (4A3467).

We analyzed the effects of steps in RNA in situ hybridization (ISH) procedures on morphology and hybridization signal with reflection-contrast microscopy (RCM) and transmission electron microscopy (TEM). In chessboard experiments, a range of fixatives containing formaldehyde, glutaraldehyde, or both, and various permeabilization protocols, including ethanol and pepsin treatment, were investigated. A transfected rat fibroblast cell line that harbors an inducible human cytomegalovirus immediate early (IE) transcription unit, and specific probes for 28S ribosomal RNA and IE messenger RNA were used for this purpose. Probes were labeled with digoxigenin and hybrids were detected with anti-digoxigenin F(ab)₂ fragments conjugated to horseradish peroxidase, followed by diaminobenzidine/H₂O₂ reaction. Effects of fixation and pre-treatments on RNA detection efficiency and morphology were monitored by RCM on whole cells. After

Epon embedding and ultra-thin cross-sectioning, the corresponding TEM images were obtained. With the pre-treatments analyzed, it appeared impossible to find an acceptable balance between ISH signals and preservation of ultrastructural morphology: when good signal-to-noise ratios are obtained, the ultrastructural morphology is already deteriorated. We discuss the parameters that influence the fragile balance between high RNA detection efficiency and good preservation of ultrastructure and the benefit of RCM monitoring in the development and procedures for pre-embedding electron microscopic ISH. (*J Histochem Cytochem* 43:665-674, 1995)

KEY WORDS: In situ hybridization; Reflection-contrast microscopy; Transmission electron microscopy; Pre-embedding; 28S rRNA; Human cytomegalovirus immediate early mRNA; Rat 9G cells; Cytochemistry.

Introduction

Light microscopic (LM) in situ hybridization (ISH) expertise gathered thus far strongly indicates that measures to increase accessibility of RNA targets, such as proteolytic pre-treatment, are often crucial for obtaining a good hybridization signal-to-noise ratio. The strength in which such measures have to be taken proved to be dependent on the extent of cross-linking during the primary fixation (1-3). In general, they compromise morphology, and often a workable balance between morphology and ISH signal must be found

experimentally. Cytochemical data that give insight into the underlying events that determine this balance are very useful in the development of non-radioactive RNA ISH procedures at both the LM and electron microscopic (EM) levels. Thus far, these data are scattered over the literature.

In ISH techniques for transmission electron microscopy (TEM), the problem of inaccessibility is even more prominent because the preservation of ultrastructure requires stronger cross-linking than is generally used for LM. In developing EM ISH procedures, two approaches can be taken: post-embedding and pre-embedding. In post-embedding EM ISH, the problem of inaccessibility is believed to be solved to a large extent by ultra-thin sectioning of the cells or tissues of interest. For plastic-embedded material, only nucleic acid targets exposed at the surface will be accessible (4), whereas for frozen sections it is claimed that targets through the entire depth of the section are available (5,6). In pre-embedding EM ISH, gaining accessibility to nucleic acid targets while maintaining ultrastructural morphology pose major problems.

¹ Supported by The Netherlands Organization of Scientific Research, Department Medical Sciences (NWO-MW), grant no. 900-534-079.

² Correspondence to: Merryn V.E. Macville, Dept. of Cytochemistry and Cytometry, U. of Leiden, Sylvius Laboratories, Wassenaarseweg 72, 2333 AL Leiden, The Netherlands.

³ Present address: Dept. of Cell Biology and Histology, U. of Nijmegen, Nijmegen, The Netherlands.

To find a workable balance, if any, between preservation of ultrastructural morphology and RNA detection efficiency in pre-embedding EM ISH, extensive experimentation, in which fixation and permeabilizing pre-treatments are the major variables, is necessary. Such experimentation would benefit considerably from a LM technique that on the one hand would permit sensitive detection of the final reaction product of an ISH procedure and on the other hand would give an indication of the ultrastructural morphology of the cells. For this purpose, reflection-contrast microscopy (RCM) was selected in combination with peroxidase/diaminobenzidine (DAB) detection. Because RCM is extremely sensitive in detecting the DAB precipitate (7-11), RCM evaluation before embedding would permit selection of the conditions under which good signal-to-noise ratios are achieved. Next to this, RCM interference patterns of unstained cells would give an indication to which extent morphology is preserved (12; see also Discussion). To establish a correlation between RCM images on the one side and subcellular morphology and RNA detection efficiency on the other, we analyzed ultra-thin cross-sections with TEM.

Materials and Methods

Cell Culture. For RCM and brightfield LM, rat 9G fibroblasts and HeLa cells were grown overnight to subconfluency on sterilized glass slides in Dulbecco's minimal essential medium supplemented with 10% (v/v) fetal calf serum at 37°C in a 5% CO₂ atmosphere. For pre-embedding EM, cells were grown on polystyrene 6-well culture plates (type 3506; Costar Europe, Badhoevedorp, The Netherlands) under the same conditions. Immediate early (IE) messenger RNA (mRNA) expression was induced in about 30% of the rat 9G cell population by addition of 50 µg/ml cycloheximide (Sigma; St Louis, MO) for 5 hr at 37°C to exponentially growing cells (13).

Nucleic Acids and Labeling. For detection of IE mRNA in rat 9G cells a plasmid probe was used, containing the 5 KB *Spb1-Sa/I* fragment of the transfected human cytomegalovirus (HCMV) IE region (13,14). For detection of ribosomal RNA (rRNA) a 2.1 KB insert specific for the 3' site of human 28S rRNA was cloned in pGEM plasmid (15,16). As negative control, a pKUN plasmid was used containing the 1 KB transcript of the caudodorsal cell hormone (CDCH) gene of the pond snail *Lymnaea stagnalis* (17). Probes were labeled with digoxigenin-11-dUTP (Boehringer-Mannheim; Mannheim, Germany) by nick-translation and were purified by Sephadex G50 (Pharmacia Biotech; Woerden, The Netherlands) gel filtration. Fragment length of labeled probes was 100-400 BP as estimated by Southern blotting.

Fixations and Pre-treatments. After culturing, cells were washed briefly at room temperature (RT) with Ringer's PBS, pH 7.4 (1.4 mM Na₂HPO₄/NaH₂PO₄, 150 mM NaCl, 4 mM KCl, 2.2 mM CaCl₂) and fixed for 30 min at RT in either 4% (v/v) formaldehyde/5% (v/v) acetic acid in PBS (136 mM NaCl, 2.7 mM KCl, 8.4 mM Na₂HPO₄, 0.9 mM KH₂PO₄, pH 7.4), 1% (w/v) formaldehyde in 0.1 M Na₂HPO₄/NaH₂PO₄ pH 7.2, 1% (w/v) formaldehyde with 0.05% or 0.5% (v/v) glutaraldehyde (EM grade; Fluka Chemie; Buchs, Switzerland) in 0.15 M NaHCO₃ pH 8.6 (18), or 1% glutaraldehyde in 0.14 M sodium cacodylate buffer, pH 7.2. All fixatives were freshly prepared before use. After fixation, cells were pre-treated with a permeabilizing agent, including ethanol, pepsin, or both. Ethanol pre-treatment was performed by dehydration in a 70-90-100% series of ethanol at RT or overnight storage in 70% ethanol at 4°C. Pepsin digestion was in 0.1% (w/v) pepsin (Sigma)/10 mM HCl, pH 2.0, at 37°C for 5, 10, or 20 min. Consecutively, cells were post-fixed in 1% formaldehyde/PBS for 10 min and blocked for fixation-induced free aldehydes in 1% (w/v)

hydroxylammonium chloride/PBS for 10 min. In between the steps, cells were rinsed in RNase-free PBS.

In Situ Hybridization. The hybridization buffer for RCM and EM consisted of 60% deionized formamide, 2 × SSC (0.3 M NaCl, 0.03 M sodium citrate), 25 mM NaH₂PO₄, 10 mM EDTA, pH 7.4, 100 µg/ml herring sperm DNA, 100 µg/ml yeast transfer RNA. Hybridization conditions were as described (3,19). For EM experiments performed on polystyrene 6-well plates, 10 µl hybridization mixture, with a final probe concentration of 5 ng/µl, was covered with a 20 × 20-mm piece of parafilm. Negative controls consisted of hybridizations without probe or with a nonspecific probe, pre-treatment of cells with RNase A (100 µg/ml in 2 × SSC) before hybridization for 30 min at 37°C, and hybridization on non-induced rat 9G cells or HeLa cells.

Hybrid Detection. Digoxigenin-labeled RNA-DNA hybrids were detected with peroxidase-conjugated anti-digoxigenin F(ab)₂ fragments (Boehringer-Mannheim) diluted 1:250 in 100 mM Tris-HCl, 600 mM NaCl, pH 7.4, containing 0.5% (w/v) blocking reagent (Boehringer-Mannheim) and, optionally, 2 mM vanadyl ribonucleoside complex (Gibco BRL/Lifetechnologies; Breda, The Netherlands) for 2 hr at 37°C. Afterwards, cells were rinsed in 100 mM Tris-HCl, 150 mM NaCl, pH 7.4. For visualization of peroxidase label, cells were incubated at RT for 20 min in the dark with 0.5 mg/ml DAB in 50 mM Tris-HCl, pH 7.4, containing 10 mM imidazole and 0.005% (v/v) H₂O₂. Before RCM monitoring or TEM processing, DAB-stained cells were post-fixed with 2% (v/v) glutaraldehyde in 0.15 M NaHCO₃ for 30 min at RT, rinsed in PBS three times for 5 min, and osmified in 1% (v/v) OsO₄ in Millonig's phosphate (0.16 M NaH₂PO₄/0.63 M NaOH, pH 7.3) for 30 min at 4°C.

Reflection-contrast Microscopy. A Leitz Orthoplan microscope (Ernst Leitz; Wetzlar, Germany) equipped for epi-illumination was adapted for RCM. The principle of this type of microscopy has been described previously (7,9,20). After dehydration, whole cells were observed using immersion oil between objective and slide without a coverslip. For reproduction reasons, all RCM micrographs shown in this article were taken from glass slides. Polystyrene caused a gray reflection at the polystyrene-immersion oil interface, whereas glass gave a completely black background. Unlike glass, polystyrene was not resistant to long exposure to immersion oil. Therefore, the wells were rinsed in 100% ethanol immediately after RCM monitoring. The monitored cells or their duplicates were further processed for TEM. For RCM examination of ultra-thin cross-sections, specimens were mounted on poly-L-lysine-coated glass slides and examined for hybridization signals. All RCM micrographs were taken on 100 ASA daylight color film.

Resin Embedding and Electron Microscopy. Cells were dehydrated and infiltrated with gradually increasing concentrations of Epon in ethanol according to standard procedures. On 6-well plates, a small volume of resin was equally distributed over each well. After overnight polymerization at 60°C, ~1-mm thin disks containing the cells were broken from the wells and re-embedded in Epon for cross-sectioning. Ultra-thin sections (60-90 nm) were cut with a diamond knife on a Reichert Ultracut E and mounted on carbon-coated collodion films on copper grids. Cells were examined with a Philips EM 410LS operating at 60 or 80 kV.

Results

The influence of different ISH protocols on cell morphology and RNA detection efficiency was investigated by evaluating results with both RCM and TEM. To observe ISH results by both types of microscopy, cells had to be transferred from an LM to an EM examining mode. Polystyrene 6-well culture plates were suitable substrates for this purpose. In our hands, the same ISH results were obtained

Table 1. Influence of ethanol on morphology and ISH results in correlation with primary fixation observed in rat 9G cells by RCM and TEM^a

Ethanol	Fixation ^b	Morphology ^c		28S rRNA signal intensity ^d		RCM IE mRNA signal	
		RCM	TEM	RCM	TEM	Intensity ^e	Percentage ^{e,f}
Without	4% FA/5% HAc	±	---	±	-	-	0
	1% FA	+	+	+	-	+	5
	1% FA/0.05% GA	++	++	±	-	-	0
	1% FA/0.5% GA	+++	++	±	-	-	0
	1% GA	+++	++	-	-	-	0
With	4% FA/5% HAc	±	----	+	-	-	0
	1% FA	+	--	+	-	+	5
	1% FA/0.05% GA	++	±	±	-	-	0
	1% FA/0.5% GA	+++	±	±	-	-	0
	1% GA	+++	±	-	-	-	0

^a RCM, reflection-contrast microscopy; TEM, transmission electron microscopy.

^b FA, formaldehyde; GA, glutaraldehyde; HAc, acetic acid.

^c RCM; + + +, concentric colors over 60% of the cell; + +, 40% concentric colors; +, 20% concentric colors; ± colored speck over cell center, gray periphery. TEM; + +, well-preserved ultrastructure; +, fairly well-preserved ultrastructure; ±, no organelles, cell mass retained; --, no organelles, loss of cell mass; ---, cell damage or extracted cells; ----, severe loss of cell mass.

^d 28S rRNA ISH signal intensity: +, clear DAB in cytoplasm; ±, weak DAB spots in cytoplasm; -, no DAB.

^e IE mRNA ISH signal intensity: +, clear DAB in cytoplasm; -, no DAB.

^f Percentage of cells showing IE mRNA ISH signal (maximum is 30%).

on glass slides and polystyrene 6-well plates. After RCM monitoring, cells were transferred into Epon blocks without cell loss or damage.

The data were obtained from rat 9G fibroblasts that were hy-

bridized immediately after primary fixation (Table 1) or treated before ISH with ethanol (Table 1), pepsin (Table 2) or ethanol and pepsin (Table 3). In general, the RNA detection efficiency appeared strongly correlated to the state of subcellular morphology. Further-

Table 2. Influence of pepsin digestion without prior ethanol treatment on the morphology and ISH results in rat 9G cells, in correlation with the primary fixation as observed by RCM and TEM^a

Fixation ^b	Pepsin time	Morphology ^c		28S rRNA signal intensity ^d		RCM IE mRNA signal	
		RCM	TEM	RCM	TEM	Intensity ^e	Percentage ^f
4% FA/5% HAc	5'	-	----	++	++	+	20
	10'	--	----	+++	+++	++	30
	20'	---	<i>g</i>	+++	<i>g</i>	++	30
1% FA	5'	----	<i>b</i>	+++	<i>b</i>	++	20
	1% FA/0.05% GA	5'	---/ + + <i>i</i>	--/ + + <i>i</i>	+ <i>j</i>	+ <i>j</i>	+ <i>j</i>
1% FA/0.05% GA	10'	---/ + + <i>i</i>	---/ + + <i>i</i>	+ <i>j</i>	+ <i>j</i>	+ <i>j</i>	20
	20'	---/ ± <i>i</i>	<i>g</i>	+	<i>g</i>	+	30
	1% FA/0.5% GA	5'	--/ + + <i>i</i>	--/ + + <i>i</i>	+ <i>j</i>	+ <i>j</i>	+ <i>j</i>
1% FA/0.5% GA	10'	---/ + + <i>i</i>	--/ + + <i>i</i>	+ <i>j</i>	+ <i>j</i>	+ <i>j</i>	5
	20'	---/ + <i>i</i>	<i>g</i>	+ <i>j</i>	+ <i>j</i>	+ <i>j</i>	10
	1% GA	5'	--/ + + + <i>i</i>	--/ + + <i>i</i>	+ <i>j</i>	+ <i>j</i>	+ <i>j</i>
1% GA	10'	---/ + + + <i>i</i>	--/ + + <i>i</i>	+ <i>j</i>	+ <i>j</i>	± <i>j</i>	5
	20'	---/ + + <i>i</i>	<i>g</i>	+ <i>j</i>	<i>g</i>	+ <i>j</i>	10

^a RCM, reflection-contrast microscopy; TEM, transmission electron microscopy. Nuclear and nucleolar ISH signals were occasionally examined by brightfield LM because DAB could sometimes be present in such large amounts that the reflection properties were lost (see text).

^b FA, formaldehyde; GA, glutaraldehyde; HAc, acetic acid.

^c RCM, morphology: + + +, concentric colors over 60% of the cell; + +, 40% concentric colors; +, 20% concentric colors; ± colored specks over cell center, gray periphery. -, predominantly gray cells; --, gray cells; ---, cell damage; ----, severe cell damage. TEM morphology: + +, well-preserved ultrastructure; --, no organelles, loss of cell mass; ---, cell damage or extracted cells; ----, severe loss of cell mass.

^d + + +, strong DAB in cytoplasm and nucleoli; + +, clear DAB in cytoplasm and nucleoli; +, clear DAB in cytoplasm.

^e + +, clear DAB in cytoplasm and nucleoplasm; +, clear DAB in cytoplasm; ±, weak DAB spots in cytoplasm.

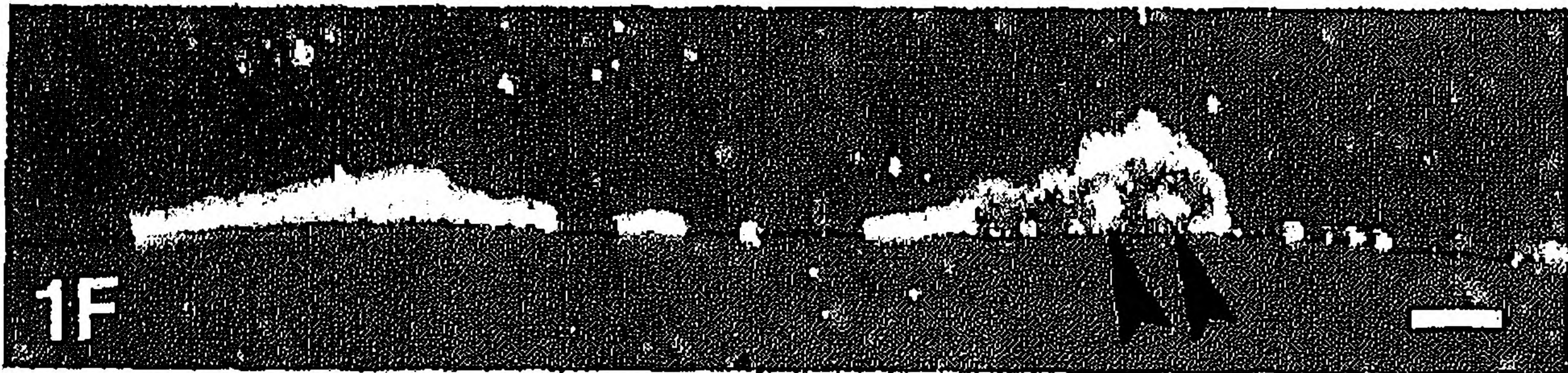
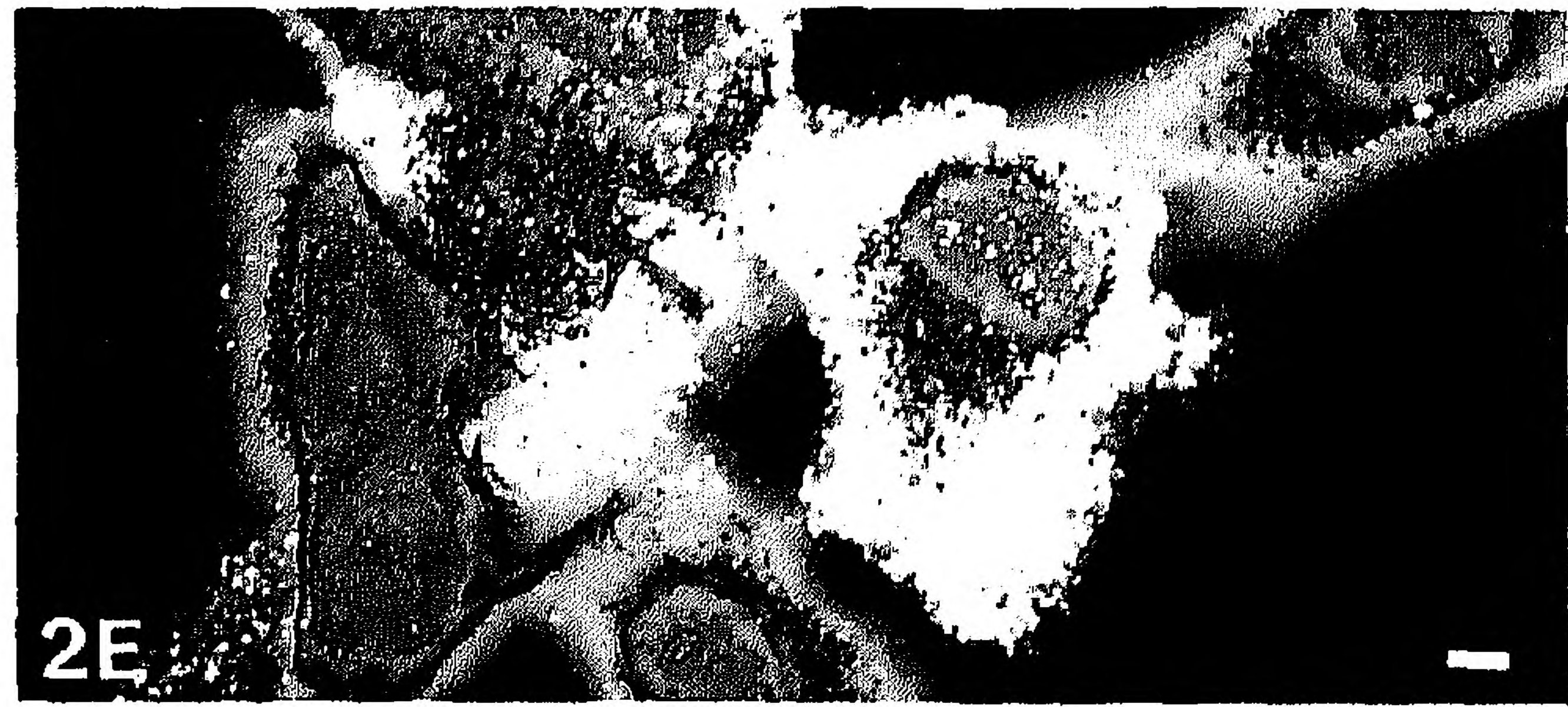
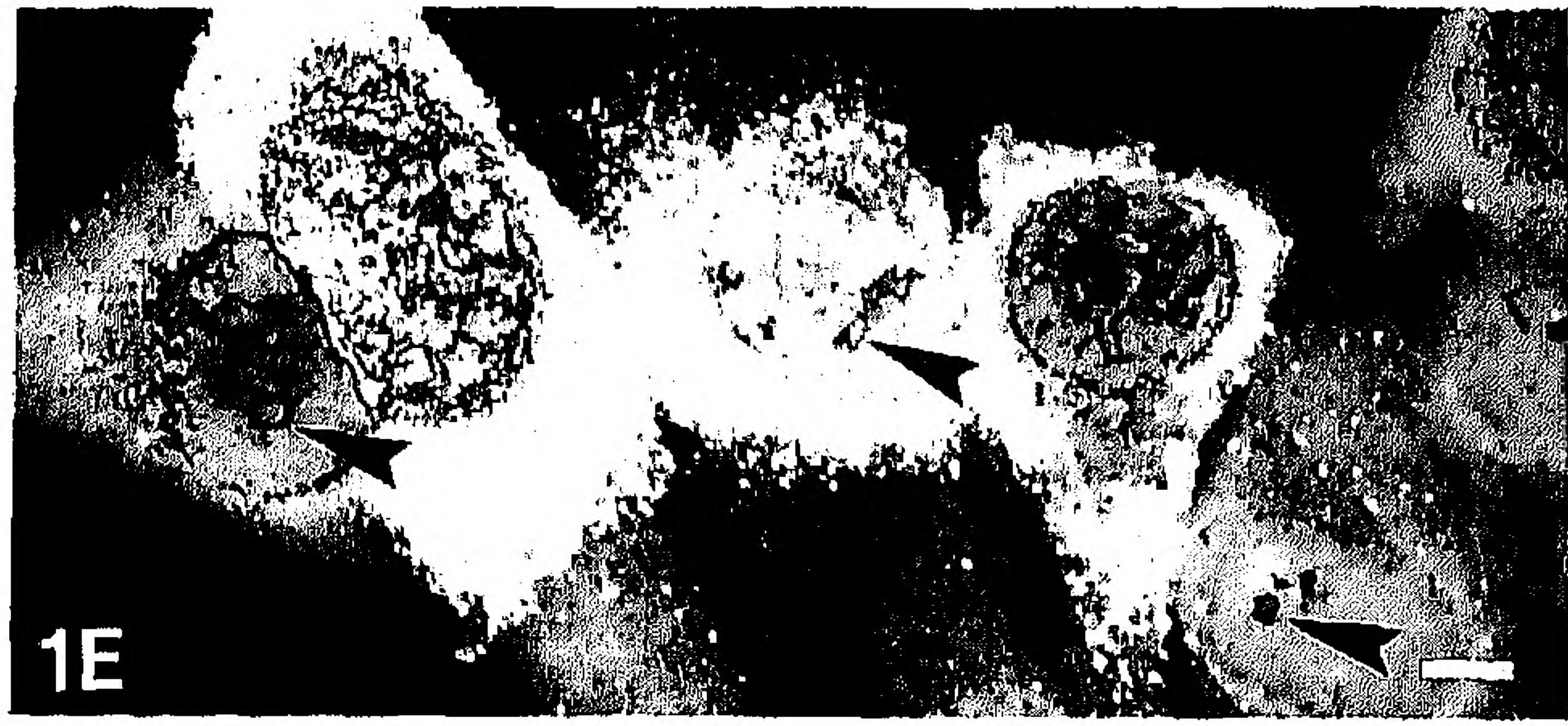
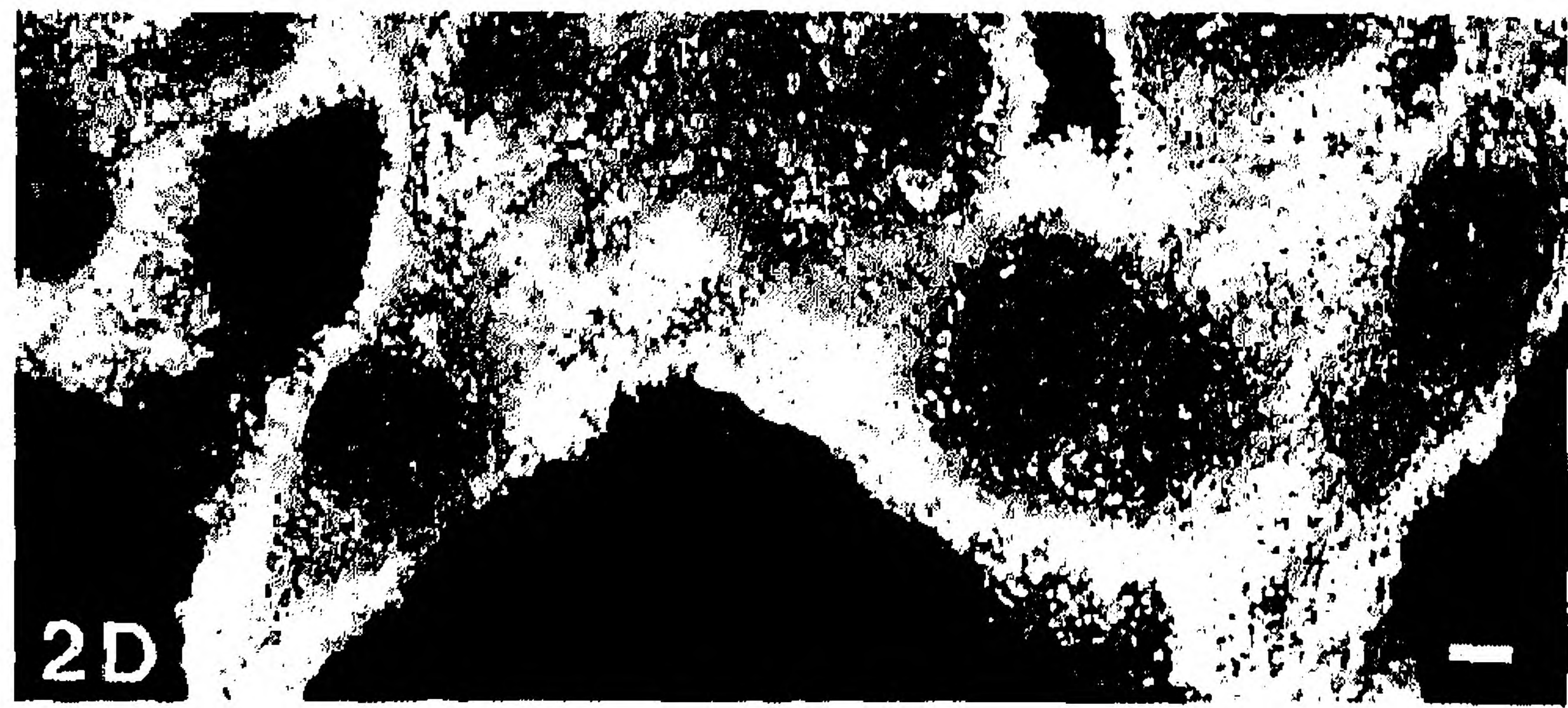
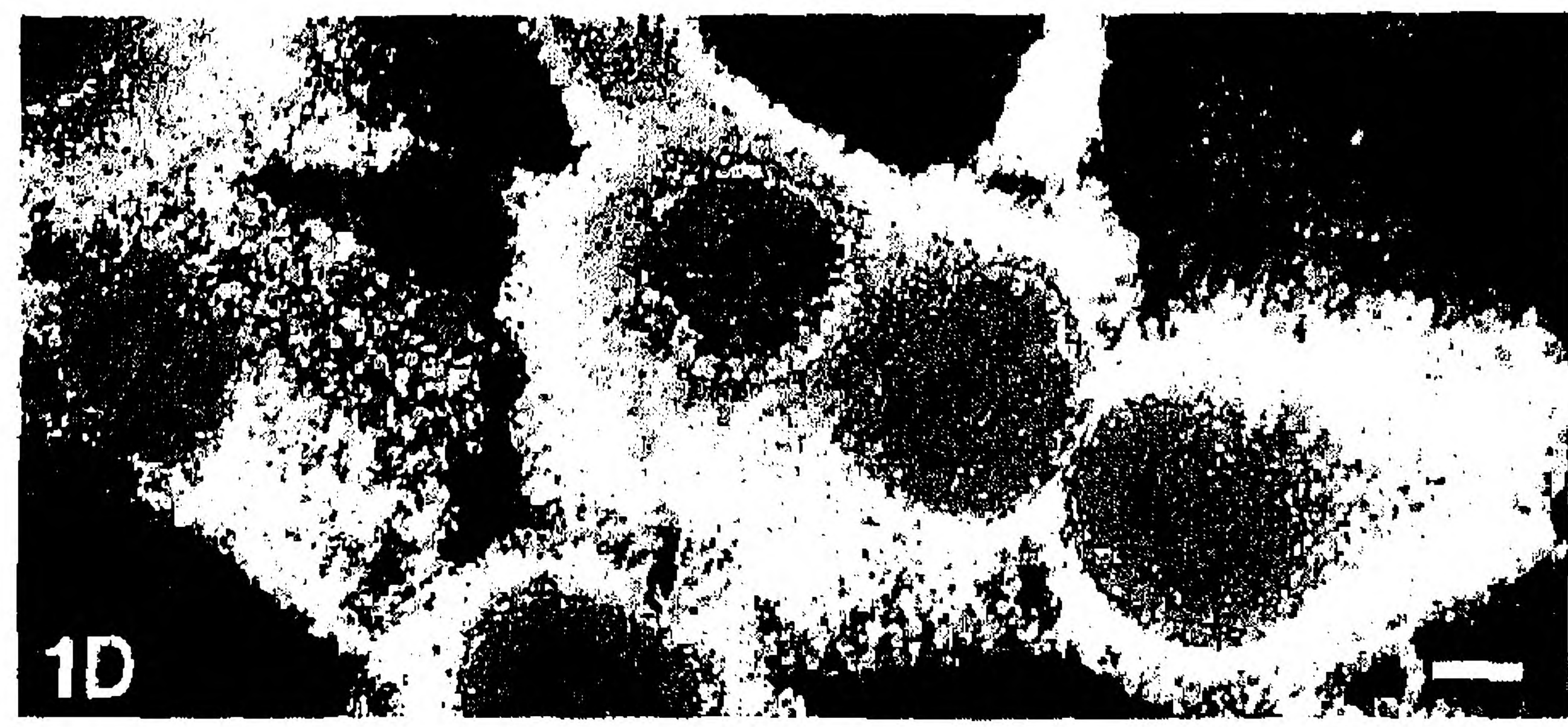
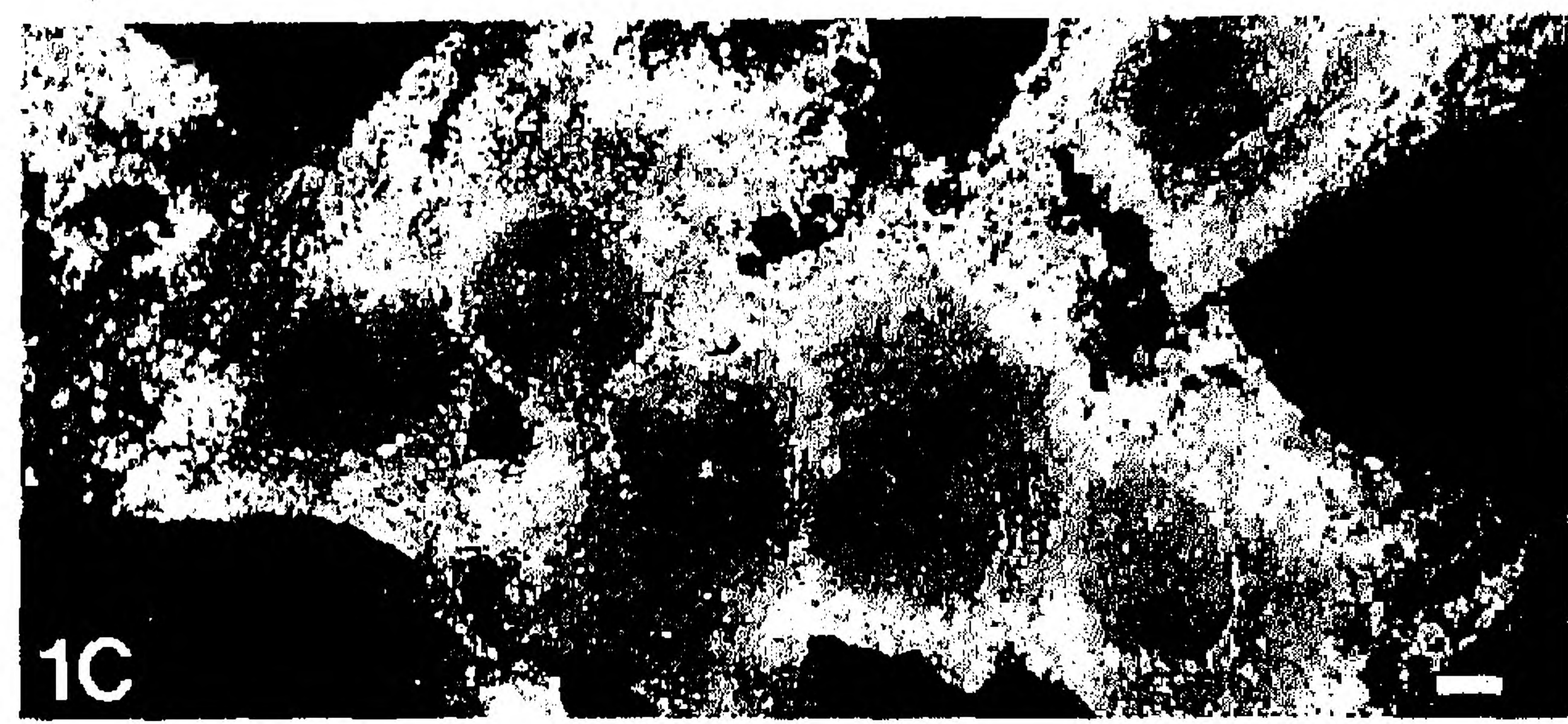
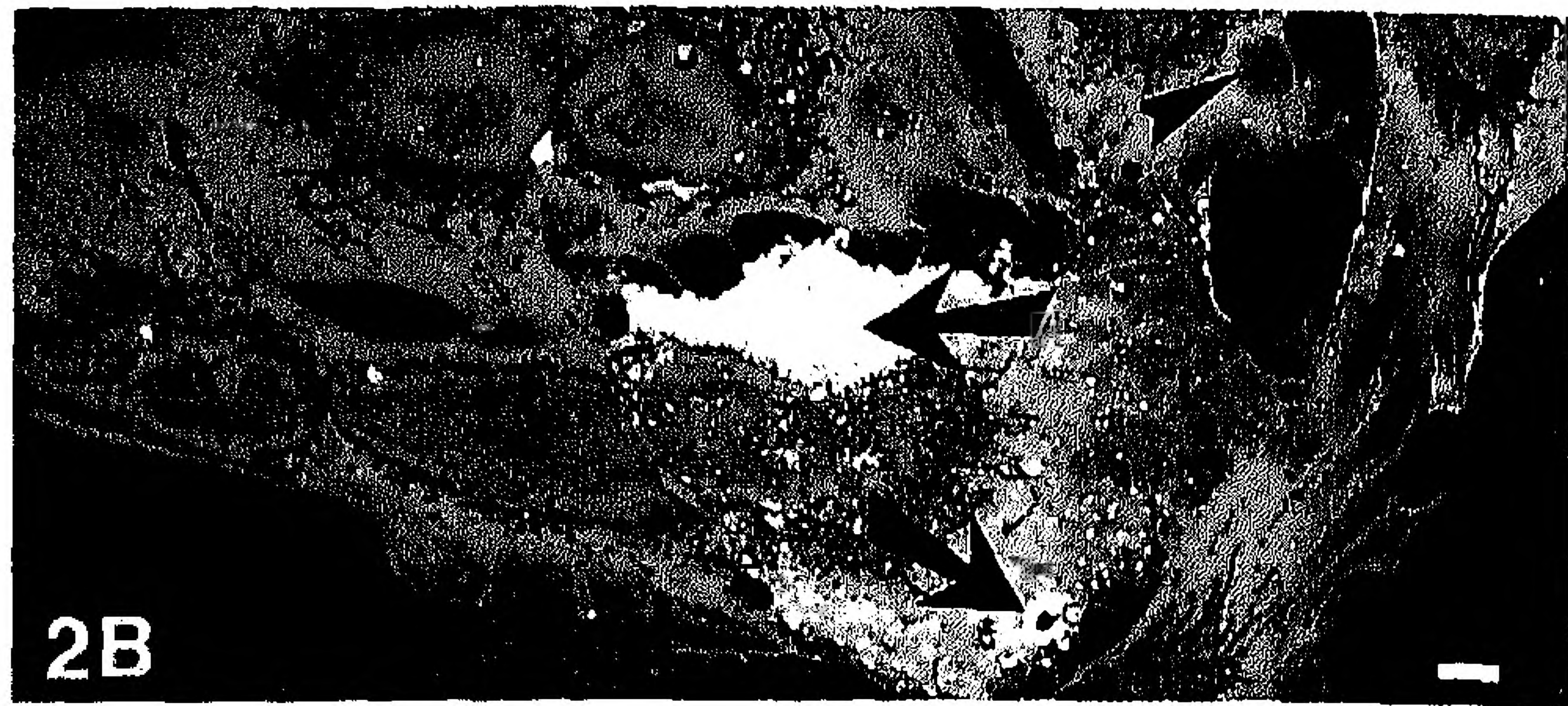
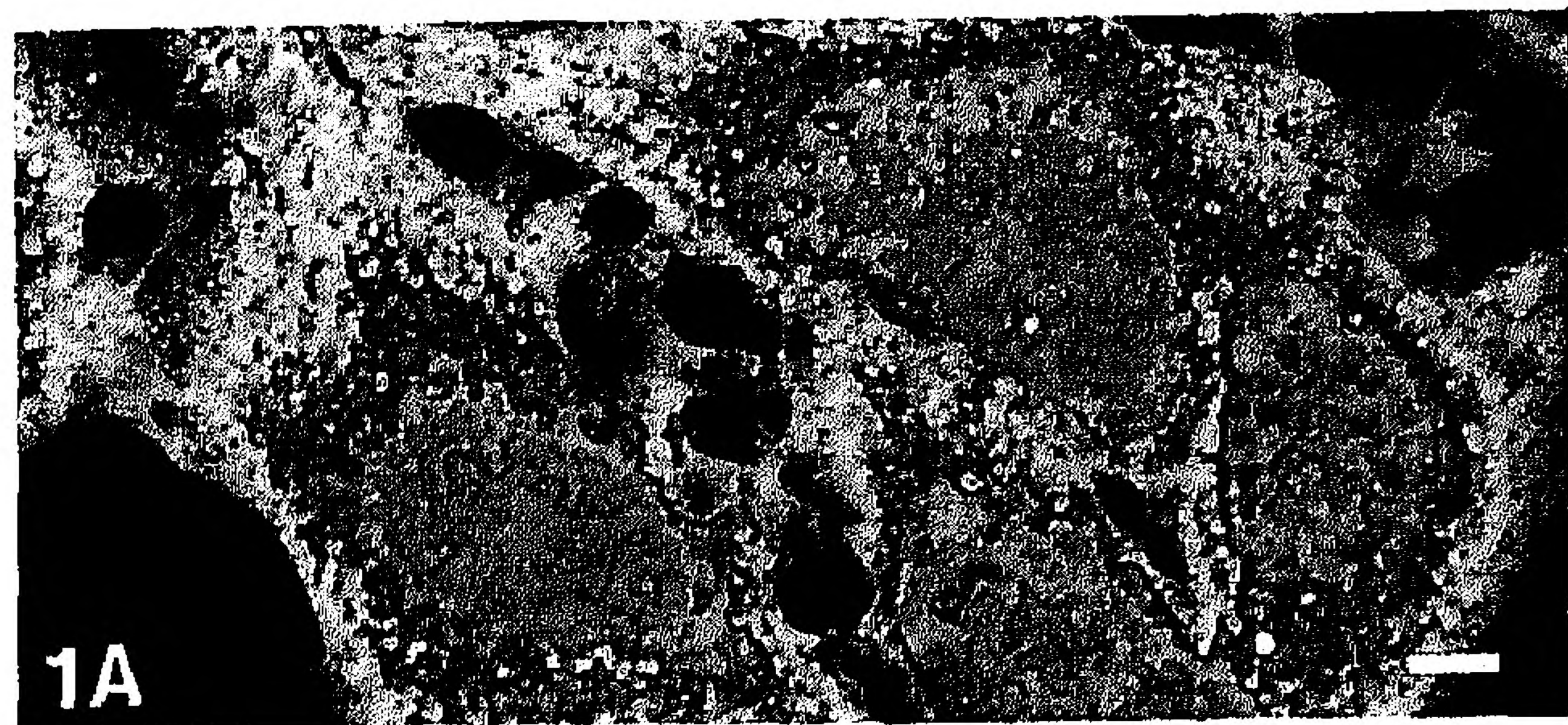
^f Percentage of cells showing IE mRNA ISH signal (maximum is 30%).

^g No data.

^h Severe cell loss.

ⁱ Heterogeneous morphology pattern within one cell, showing distinct disrupted parts (indicated left of slash) and preserved parts (indicated right of slash).

^j Heterogeneous (patchy) signal pattern within one cell, showing parts with ISH signal (indicated) and parts without ISH signal.



more, by evaluating RCM data with corresponding TEM data, we were able to use RCM images to predict results at the ultrastructural level to a large extent.

Monitoring Morphology and 28S rRNA ISH Signals by RCM and TEM

Effects of Fixation. The RCM image of 4% formaldehyde/5% acetic acid-fixed cells (Figure 1A) showed a blue and brown speckled interference pattern over the central region surrounded by a grayish-white area. The corresponding TEM image (Figure 3A) revealed extracted cells in which only nuclei and nucleoli were recognized.

Cells fixed with 1% formaldehyde showed a regular pattern of concentrically arranged colors over the center of the cell. In TEM, the ultrastructural morphology was fairly well preserved. The use of glutaraldehyde during primary fixation optimized the preservation of ultrastructural morphology. For example, 1% formaldehyde/0.5% glutaraldehyde-fixed cells showed a dense nucleus and good preservation of membrane structures in the cytoplasm (similar to Figure 4A). The corresponding RCM image (Figure 2A) showed an interference pattern of concentrically arranged colors over 60% of the cell: purple and green in the center, then changing from yellow to blue, brown, and grayish-white towards the outer periphery.

Effects of Hybridization. The influence on morphology of the hybridization step itself was of primary interest because this step is indispensable in the ISH protocol and is performed over a long period in a predominantly organic environment of formamide. To investigate this, rat 9G cells were fixed and hybridized overnight in the absence of probe (pseudohybridization) without preceding treatments (upper half of Table 1). In all types of fixation, cell morphology in RCM and TEM did not differ from cells that were not hybridized at all. When the cell morphology was affected by permeabilization treatments, the hybridization step did not deteriorate the morphology any further. In addition, immunocytochemical steps did not influence cell morphology.

When ISH was performed without any preceding treatment, signals for 28S rRNA were visible in RCM as clear spots in the cytoplasm of cells fixed with 4% formaldehyde/5% acetic acid (Figure 1B) or 1% formaldehyde. The 28S rRNA ISH signal intensity decreased as glutaraldehyde concentration of the fixation increased. In TEM, for all fixatives, no 28S rRNA ISH signals were visible.

Effects of Ethanol. The influence of ethanol in the ISH protocol on the morphology was investigated by comparing cells that were either gradually dehydrated in 70–90–100% ethanol or stored overnight in 70% ethanol at 4°C before hybridization with cells that were hybridized directly after fixation (Table 1). For all types of fixation, the RCM interference color pattern did not alter after ethanol treatment. TEM examination, however, revealed deterioration of ultrastructural morphology for all fixatives, especially in cells fixed with formaldehyde, glutaraldehyde, or both. Cells fixed with 1% formaldehyde/0.5% glutaraldehyde and pre-treated with ethanol revealed a considerable loss of organelle architecture: mitochondria, endoplasmic reticulum, Golgi apparatus, and vesicles were vaguely discernible. Still, the cell mass and volume was retained, explaining their unaltered reflection properties.

Although ethanol pre-treatment affected the ultrastructural morphology of the cell, the ISH detection efficiency for 28S rRNA did not increase, either at the RCM or the TEM level.

Effects of Pepsin. The influence of pepsin on cell morphology was investigated in pseudohybridized cells and in IE mRNA-negative cells present in induced cell batches. Cells were fixed and then pre-treated with 0.1% pepsin for various time periods (Table 2). When 4% formaldehyde/5% acetic acid-fixed cells were pre-treated with pepsin for 5 min, they revealed an overall gray color with a blue-brown ring in the center of the cell, probably indicating the nuclear border. In the majority of cells, one to three blue-brown dots were discriminated within the ring, representing the nucleoli (similar to Figure 1E). The corresponding TEM image revealed only remnants of cytoplasm, nucleus, and nucleoli. Longer pepsin pre-treatment led to further loss of interference color and cell damage, as could be seen in RCM. In TEM, longer pepsin pre-treatment resulted in considerable loss of cell mass and cell damage.

Pepsin pre-treatment enhanced the ISH signal intensity in 4% formaldehyde/5% acetic acid-fixed cells (Table 2). In RCM, cells hybridized for 28S rRNA showed homogeneously distributed DAB precipitate over the cytoplasm (Figure 1C). Moreover, the ISH signal intensity increased after prolonged pepsin pre-treatment. Nucleoli appeared devoid of label. However, by examining the same image field with brightfield LM, DAB spots were clearly visible. This is explained by the fact that reflection properties of DAB are lost if it is present in large amounts (10). In TEM, 28S rRNA ISH signals were clearly visible over the remnants of the cytoplasm and nucleoli (similar to Figure 3B).

A relatively short pepsin digestion on 1% formaldehyde-fixed

Figure 1. RCM image of rat 9G cell monolayer fixed with 4% formaldehyde/5% acetic acid (A) directly after fixation and (B) after 28S rRNA ISH and peroxidase/DAB detection without any pre-treatment. Cells show white DAB spots over the cytoplasm. (C) After pre-treatment with pepsin for 5 min, cells show equally strong 28S rRNA ISH signals as (D) cells that were additionally pre-treated with ethanol. Nucleolar ISH signals are present (see Figure 1F) but are not visible in RCM owing to loss of reflection properties of large amounts of DAB (see text). (E) Rat 9G cells pre-treated with ethanol and pepsin for 5 min show many strong IE mRNA ISH signals. Blue-brown dots (arrowheads) represent nucleoli. (F) Ultra-thin (90-nm) cross-section of cells similarly treated as in D demonstrates 28S rRNA in cytoplasm and nucleoli (arrowheads). Bars = 5 µm.

Figure 2. RCM image of rat 9G cell monolayer fixed with 1% formaldehyde/0.5% glutaraldehyde (A) directly after fixation and (B) after pepsin pre-treatment for 5 min and IE mRNA ISH, showing heterogeneous (patchy) DAB signals (arrows). Negative cells reveal distinct black holes (arrowhead). (C) When 28S rRNA ISH is performed on similarly treated cells, a patchy pattern is observed over all cells. (D) Cells treated with ethanol before a 5-min pepsin treatment show homogeneous DAB staining in the cytoplasm of all cells after 28S rRNA ISH and (E) after IE mRNA ISH, in the cytoplasm and nucleus. (F) Ultra-thin (90-nm) cross-section of cells similarly treated as in D demonstrates DAB staining at the outer layer of the cell, indicating poor penetration of detection reagents. Bars = 5 µm.

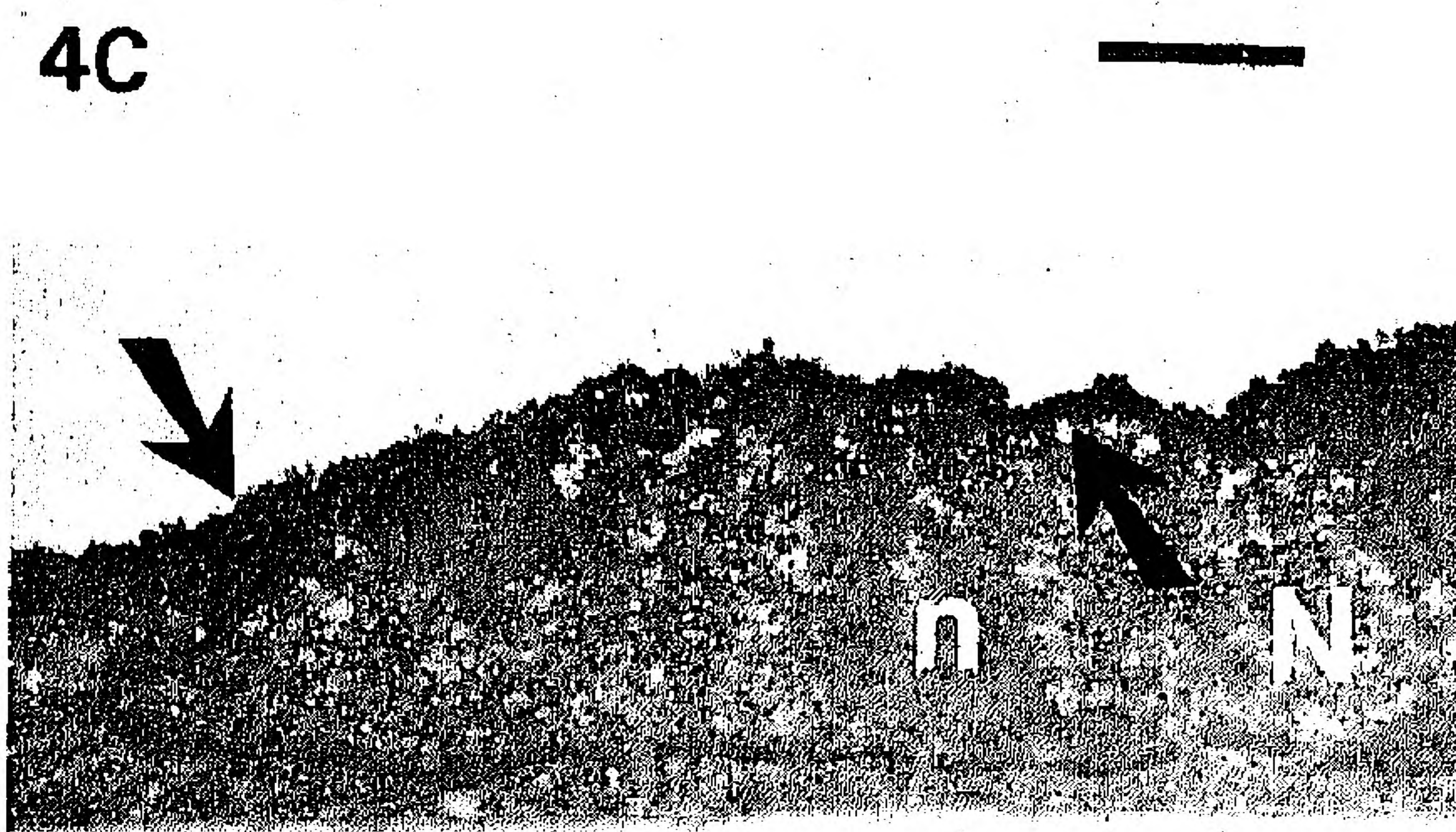
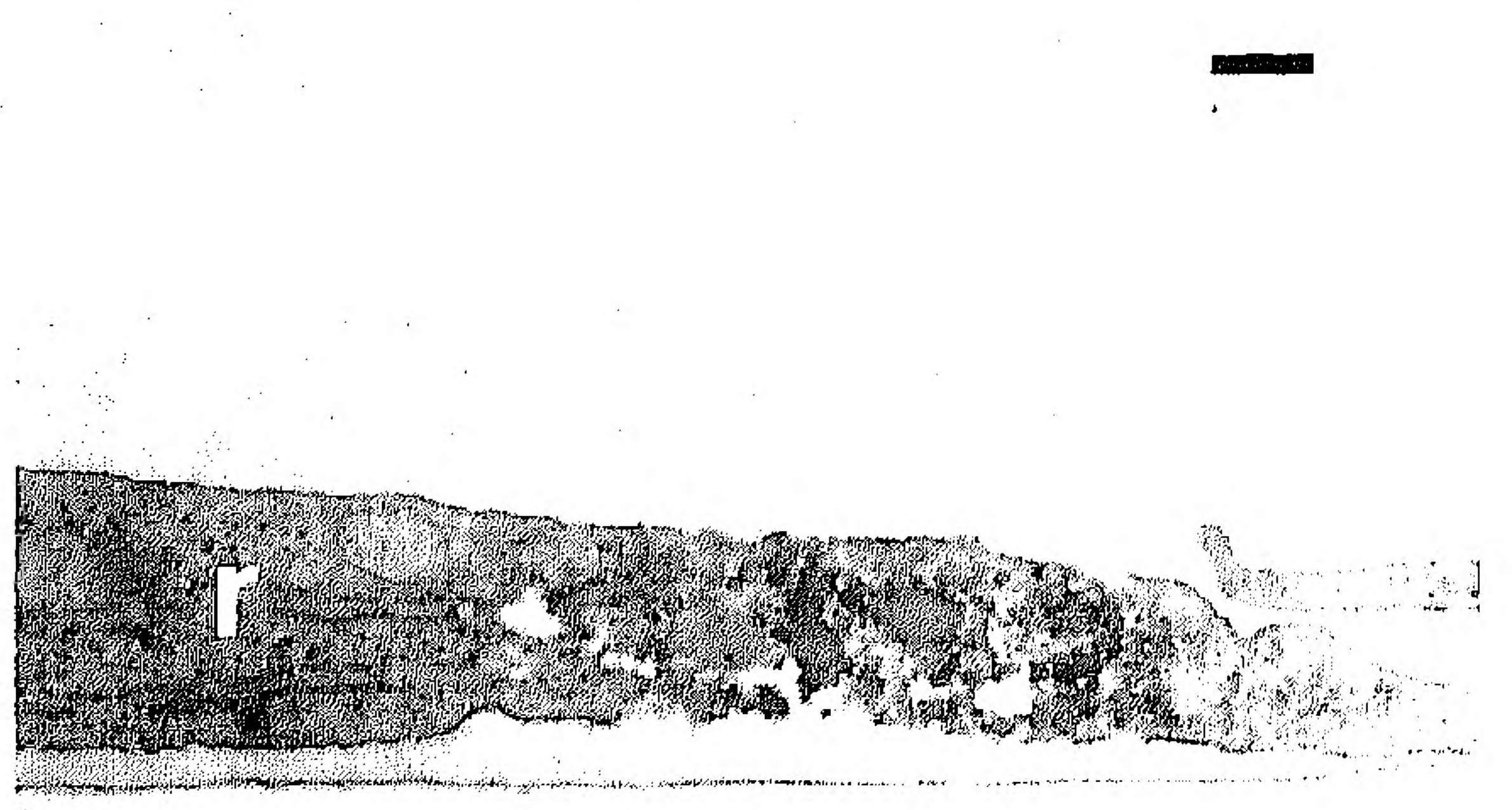
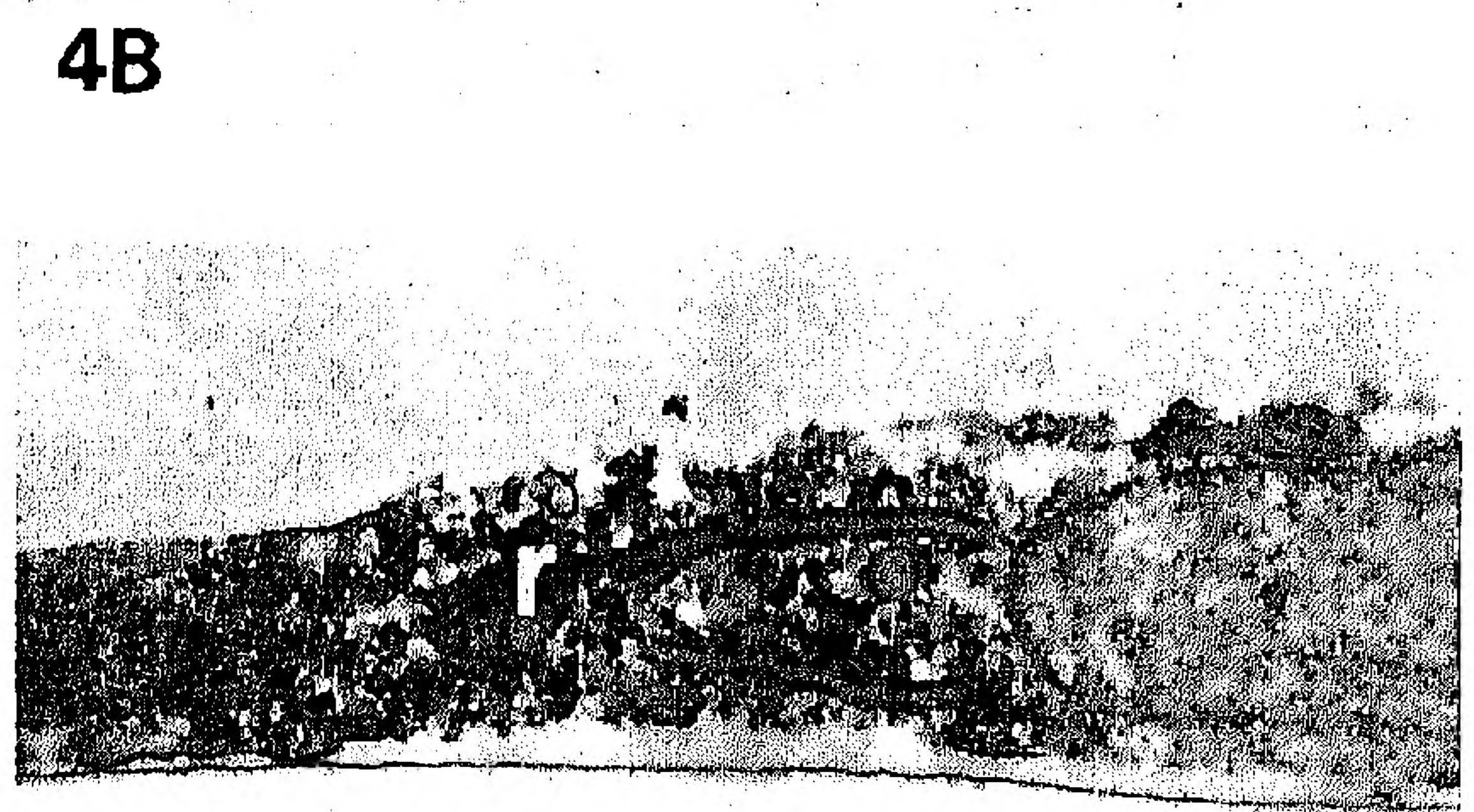
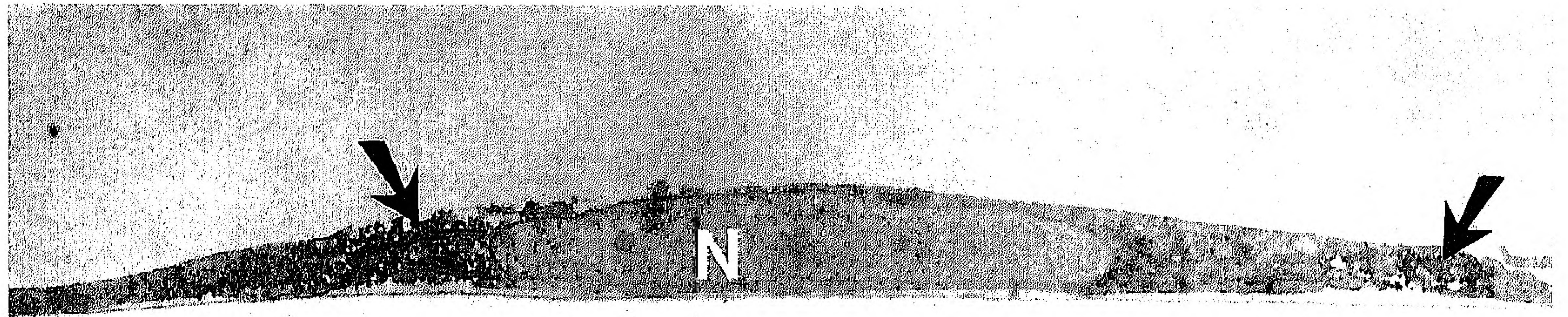
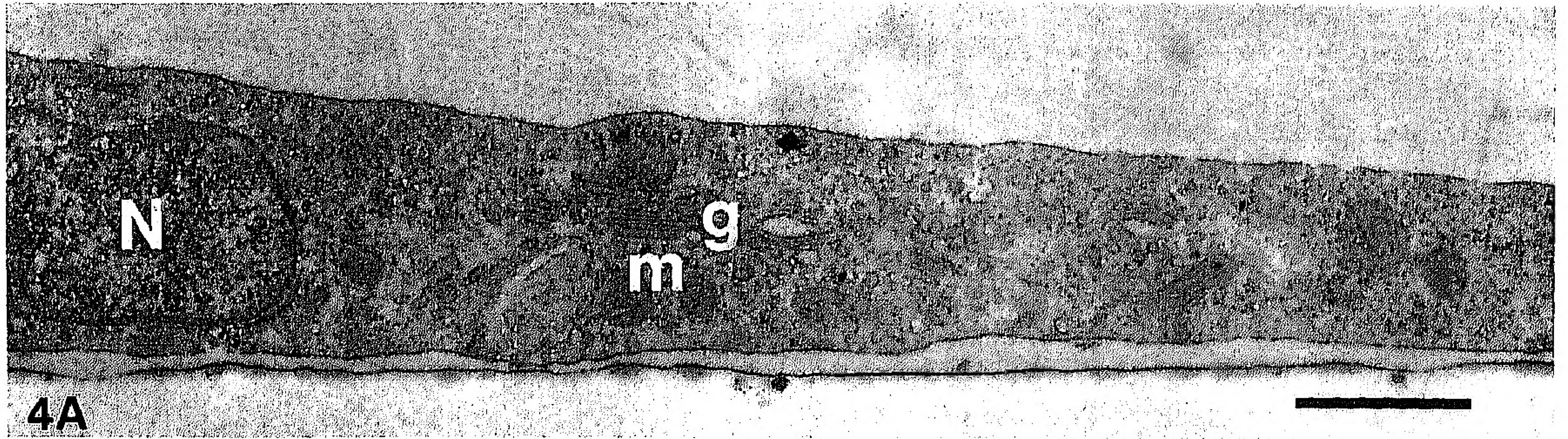
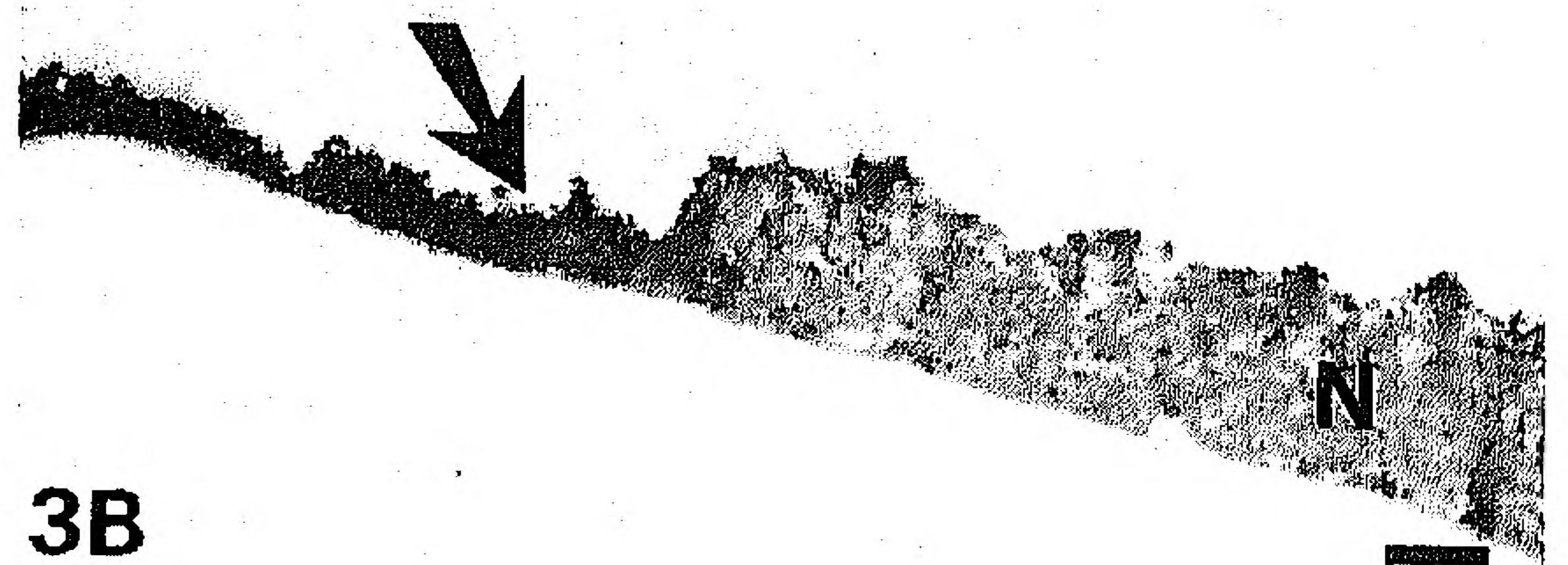
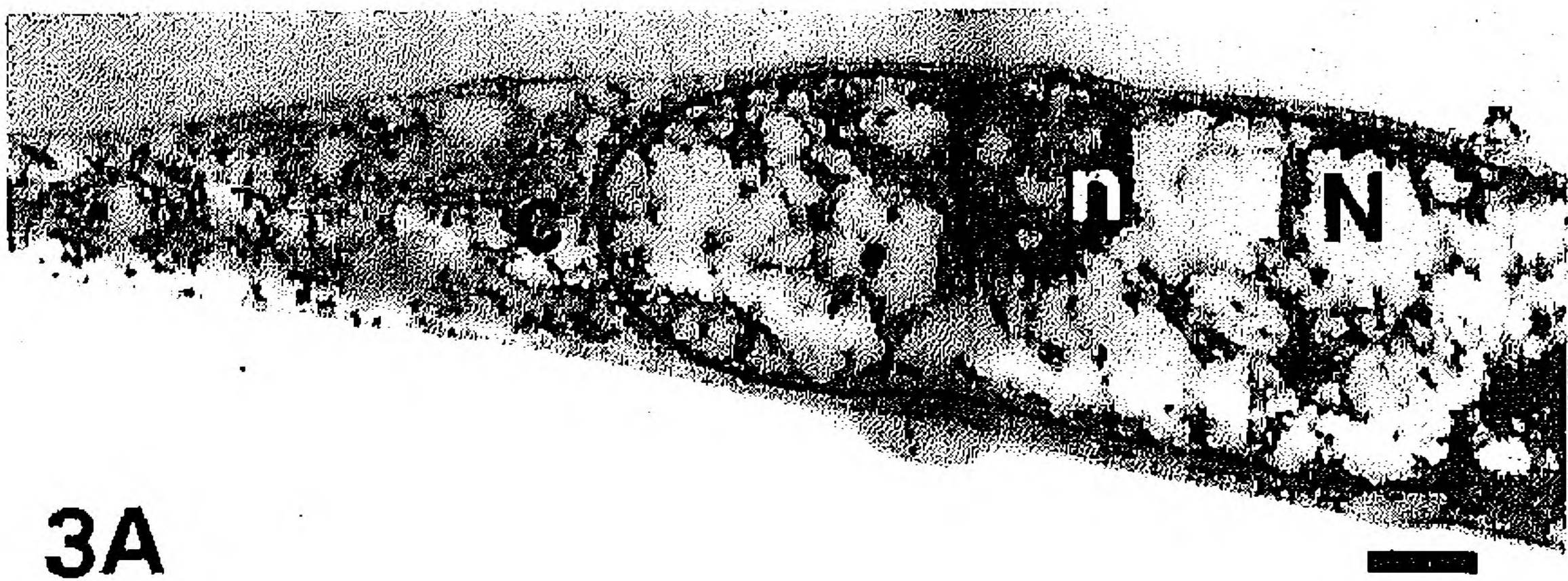


Table 3. Influence of pepsin digestion with prior ethanol treatment on the morphology and ISH results in rat 9G cells, in correlation with the primary fixation as observed by RCM and TEM^a

Fixation ^b	Pepsin time	Morphology ^c		28S rRNA signal intensity ^d		RCM IE mRNA signal	
		RCM	TEM	RCM	TEM	Intensity ^e	Percentage ^f
4% FA/5% HAc	5'	±	----	+	++	++	20
	10'	-	----	+++	+++	+++	30
	20'	--	<i>g</i>	+++	<i>g</i>	+++	30
1% FA	5'	----	<i>h</i>	+++	<i>h</i>	++	20
1% FA/0.05% GA	5'	+	-	+	± ⁱ	++	10
	10'	±	-	+	+ ⁱ	++	20
	20'	--	<i>g</i>	++	<i>g</i>	++	30
1% FA/0.5% GA	5'	++	-	+	± ⁱ	++	<5
	10'	+	-	+	+ ⁱ	++	5
	20'	-	<i>g</i>	+	<i>g</i>	++	10
1% GA	5'	++	-	±	± ⁱ	±	<5
	10'	+	-	±	± ⁱ	±	5
	20'	±	<i>g</i>	+	<i>g</i>	+	10

^a RCM, reflection-contrast microscopy; TEM, transmission electron microscopy. Nuclear and nucleolar ISH signals were occasionally examined by brightfield LM because DAB could sometimes be present in such large amounts that the reflection properties were lost (see text).

^b FA, formaldehyde; GA, glutaraldehyde; HAc, acetic acid.

^c RCM morphology: ++, 40% concentric colors; +, 20% concentric colors; ± colored specks over cell center, gray periphery. -, predominantly gray cells; --, gray cells; ----, severe cell damage. TEM morphology: -, no organelles, little loss of cell mass; ----, severe loss of cell mass.

^d + + +, strong DAB in cytoplasm and nucleoli; + +, clear DAB in cytoplasm and nucleoli; +, clear DAB in cytoplasm; ± weak DAB spots in cytoplasm.

^e + + +, strong DAB in cytoplasm and nucleoplasm; + +, clear DAB in cytoplasm and nucleoplasm; +, clear DAB in cytoplasm; ±, weak DAB spots in cytoplasm.

^f Percentage of cells showing IE mRNA ISH signal (maximum is 30%).

^g No data.

^h Severe cell loss.

ⁱ Limited penetration, showing ISH signal at the outer part of the cell (indicated) and not at other parts.

cells resulted in strong 28S rRNA ISH signals but severe cell damage, such that TEM data could not be obtained (Table 2).

The cells were more resistant to pepsin when glutaraldehyde was used in the fixative (Table 2). For example, 1% formaldehyde/0.5% glutaraldehyde-fixed cells still revealed a concentric color pattern in RCM after pepsin digestion for 5 min, but over a smaller area (Figure 2B) compared to the initial situation (Figure 2A). However, within the cell distinct black areas appeared, indicating severe damage or absence of cellular material. This was confirmed in TEM images, generally showing well-preserved cells but with disrupted areas through the entire depth of the cytoplasm. The nuclei were not affected. A pepsin pre-treatment for 5 min caused a patchy ISH signal pattern over the cytoplasm for 28S rRNA (Figure 2C), and nucleolar rRNA was not detected. In the corresponding TEM image, DAB precipitate was present at the disrupted sites in the cytoplasm (Figures 4B-4D). By increasing the time of pepsin treatment, the ISH signals became more intense and the DAB patches larger, as observed with both RCM and TEM. Nucleolar ISH signals, however, remained invisible. After pepsin pre-treatment

of 20 min, in RCM the DAB staining pattern was homogeneous, but the morphology still revealed differential disruption. Apparently RNA targets in preserved parts were accessible through the disrupted parts.

Effects of Ethanol and Pepsin. In Table 3, the influence on morphology and RNA detection efficiency of pepsin digestion after an ethanol treatment is presented. For cells fixed with 4% formaldehyde/5% acetic acid, the influence of pepsin on RNA detection efficiency was the same whether or not an ethanol pre-treatment had been used. For 28S rRNA ISH, no difference in ISH signal intensity or localization was observed in RCM (compare Figures 1C and 1D). For preservation of morphology at the RCM level, however, cells were less affected by pepsin. Examination of ultra-thin cross-sections of cells fixed with 4% formaldehyde/5% acetic acid, pre-treated with ethanol, and then with pepsin for 5 min showed intense ISH signals for 28S rRNA over the cytoplasm and nucleoli in both RCM and TEM (Figures 1F and 3B, respectively).

In 1% formaldehyde-fixed cells, no beneficial effect of addi-

Figure 3. TEM images of cross-sectioned rat 9G cells fixed with 4% formaldehyde/5% acetic acid (A) directly after fixation and (B) hybridized for 28S rRNA after ethanol pre-treatment and pepsin digestion for 5 min. DAB signals are present over the cytoplasm (arrow) and nucleoli (shown in Figure 1F). N, nucleus; n, nucleolus; c, cytoplasm. Bars = 0.5 µm.

Figure 4. TEM images of cross-sectioned rat 9G cells fixed with 1% formaldehyde/0.5% glutaraldehyde (A) after pseudohybridization and (B) after pepsin digestion for 5 min and 28S rRNA ISH, showing DAB signals (arrows) in the disrupted cell areas. (C,D) Details of B. (E) After ethanol pre-treatment and pepsin digestion for 5 min, DAB signals (arrows) are present only in the outer layer of cells (see also Figure 2F). N, nucleus; n, nucleolus; c, cytoplasm; m, mitochondrion; g, Golgi apparatus; r, rough endoplasmic reticulum. Bars = 1 µm.

tional ethanol treatment at any microscopic level was observed (Table 3).

In formaldehyde/glutaraldehyde- and glutaraldehyde-fixed cells, ethanol pre-treatment had a remarkable effect on pepsin action (Table 3). In RCM and TEM, respectively, the black holes and differential disruption did not appear. Instead, in RCM the cell edges looked smooth and the area of concentrically arranged colors decreased. For example, in cells fixed with 1% formaldehyde/0.5% glutaraldehyde and pre-treated with ethanol, pepsin digestion for 5 min resulted in a 20% decrease of the colored area (Figure 2E) and pepsin digestion for 20 min resulted in predominantly gray cells. In TEM, flattening of the cells was observed. Moreover, the intracellular architecture of the cells was not well preserved. The influence of pepsin was more severe when cells were digested for longer periods or when they were fixed in low cross-linking fixatives, and vice versa. Cells fixed with 1% glutaraldehyde were severely damaged only after pepsin pre-treatment for >30 min (data not shown).

In ISH detection for 28S rRNA in formaldehyde/glutaraldehyde- or glutaraldehyde-fixed cells treated with ethanol and then with pepsin, the patchy DAB pattern did not occur. For example, in RCM, cells fixed with 1% formaldehyde/0.5% glutaraldehyde, pre-treated with ethanol, and then with pepsin for 5 min showed ISH signals homogeneously over the cytoplasm (Figure 2D). Nucleoli were devoid of label, as confirmed by brightfield LM and examination of ultra-thin cross-sections. Remarkably, cross-sections of these cells showed DAB staining only at the outer layer of the cell (Figures 2F and 4E) in RCM and TEM, respectively.

Monitoring of IE mRNA ISH by RCM

IE mRNA expression is cell cycle-dependent, and therefore various expression levels are present within a given cell population. The most sensitive protocol will detect all expression levels, resulting in a maximum of 30% positive cells (13). In such a case, cells expressing high levels of IE mRNA will show strong ISH signals. The sensitivity of the different ISH protocols could be investigated not only by monitoring IE mRNA signal intensity but also by determination of the percentage of positive cells.

In hybridizations without and with ethanol pre-treatment, IE mRNA was detected in a small percentage of 1% formaldehyde-fixed cells, whereas no IE mRNA ISH signals were observed with the other fixatives (Table 1).

After pepsin treatment for 5 min, 20% IE mRNA-expressing cells were detected in cells fixed with 4% formaldehyde/5% acetic acid. A maximum of 30% positive cells was achieved after pepsin treatment for 10 min (Table 2). A preceding ethanol pre-treatment did not increase the percentage but did improve the intensity of ISH signals in RCM (Figure 1E; Table 3). In brightfield LM, nuclear IE mRNA ISH signals were observed, whereas they were not observed when ethanol was not used. For cells fixed with 1% formaldehyde, as already shown for 28S rRNA ISH, RNA detection efficiency increased after pepsin treatment, but the morphology was severely damaged.

In formaldehyde/glutaraldehyde- and glutaraldehyde-fixed cells, similar to 28S rRNA ISH signals, the patchy patterns occurred when cells were pre-treated with pepsin without a prior ethanol treat-

ment (Table 2). Under the influence of pepsin, the percentage of detected IE mRNA-expressing cells increased. With an additional ethanol treatment, IE mRNA ISH signals not only were homogeneously distributed over the cytoplasm, as observed with RCM (Figure 2E) but were also present in one large spot in the nucleus, as observed with brightfield LM. The percentage of positive cells observed, however, did not increase further with ethanol pre-treatment. In cells fixed with 1% formaldehyde/0.05% glutaraldehyde, maximal sensitivity was reached after pepsin treatment for 20 min. In cells fixed with a higher glutaraldehyde concentration, however, maximal sensitivity was not reached with the investigated times of pepsin treatment.

Specificity of ISH Signals

The specificity of hybridization signals was confirmed by obtaining ISH signals without in situ denaturation of nuclear DNA and absence of signals after RNase treatment, implying that RNA was uniquely stained. No signals were observed when ISH was performed with a nonspecific probe or when non-induced rat 9G cells or HeLa cells were used (data not shown). Moreover, the presence of IE mRNA non-expressing cells in stimulated rat 9G populations provided a strong internal specificity control.

Discussion

We have used RCM and TEM to study the effects of fixations and pre-treatments as performed in RNA ISH procedures on cell morphology and hybridization signal. The results show that the lipid-dissolving action of ethanol and the protein-digesting action of pepsin, as well as their combined actions, are highly dependent on the type of primary fixation. In general, they have an adverse effect on ultrastructural morphology but a beneficial effect on hybridization signal. Pepsin digestion improved the sensitivity of the ISH procedure with all fixatives tested. The benefit of a preceding ethanol treatment was that homogeneously distributed hybridization signals were obtained and that it potentiated the pepsin effect, particularly for cells fixed with formaldehyde/glutaraldehyde fixatives. An optimal balance between hybridization signal and preservation of ultrastructural morphology was not obtained under the conditions tested: when good ISH signal-to-noise ratios were obtained, ultrastructural morphology had already deteriorated to an unacceptable extent.

The effects of ethanol and pepsin can be explained by their cytochemical properties. Ethanol dissolves lipids and precipitates proteins and nucleic acids, resulting in loss of cytoplasmic architecture (but preserved nuclei). For formaldehyde- and/or glutaraldehyde-fixed cells, the effect of ethanol on ISH signal is more prominent than for formaldehyde/acetic acid-fixed cells, probably as a consequence of loss of lipids during the formaldehyde/acetic acid fixation.

Pepsin hydrolyzes peptide bonds, leading to loss of protein mass and thereby creating a more "porous" matrix through which reagents diffuse more easily. With all fixations tested, the effect of pepsin was prominent, particularly after ethanol treatment. In formaldehyde/glutaraldehyde- and glutaraldehyde-fixed cells a patchy ISH signal pattern was demonstrated when cells were not dehydrated

or stored in ethanol before pepsin treatment. The reason for this differential disruption by pepsin is not fully understood. Probably pepsin action becomes first manifest on the weakest parts of the outer cell membrane, causing local damage. From these damaged sites, pepsin further disrupts the cytoplasm, making RNA targets more accessible for hybridization.

Image formation in RCM is based on a difference in refractive index between medium and object. Furthermore, since specimens were studied using a xenon lamp, in which all wavelengths are equally represented, changes in color may be observed. This is explained by interference phenomena of the reflected light, whereby, depending on the thickness of the reflecting layer, certain wavelengths are selectively reflected and others are suppressed.

By correlating RCM color patterns of cells to their ultrastructure in TEM, we were able to define the following criteria, from which the preservation of ultrastructural morphology can be predicted to a large extent: (a) a pattern of concentrically arranged colors indicates preservation of cell mass and volume but not necessarily preservation of organelle architecture; (b) a colorful speckled pattern indicates loss of cell mass but with preservation of cell volume (e.g., formaldehyde/acetic acid fixation); (c) loss of color diversity indicates reduction of cell mass and volume (flattening); and (d) absence of color (black) indicates severe damage or absence of cellular material. There was only one exception to the predictive value of RCM images for ultrastructural morphology: ethanol dehydration did not alter reflection properties but it had a major effect on cellular integrity. Remarkably, saponin treatment of formaldehyde- and formaldehyde/glutaraldehyde-fixed cells led to good RCM and TEM results, indicating that removal of the cholesterol component from membranes does not visibly affect ultrastructure (Macville et al., submitted for publication).

In previous studies, DAB detection with RCM proved to be a very sensitive detection method for DNA ISH (7,8) and for immunocytochemical studies (10,11). In addition, in this study very small amounts of DAB, not visible in brightfield LM, could be detected as bright individual spots. The ISH signals that were scored in RCM with "+" and "±" were hardly visible and not visible, respectively, in brightfield LM. Therefore, RCM improved the sensitivity range of RNA ISH signal detection. This enabled us to detect changes in weak ISH signals even after subtle changes in pre-treatment in cells that were strongly cross-linked during fixation.

DAB may not be the ideal marker for TEM, owing to suboptimal contrast and localization properties that obscure ultrastructural detail or reduce resolution. In principle, colloidal gold particles would be a better alternative. Colloidal gold particles with a diameter of 5 nm or more have been used in pre-embedding EM ISH studies for detection of mRNA. However, to obtain good penetration of detection reagents, ultrastructural morphology had to be compromised (21–25). The advent of ultra-small gold particles conjugated to F(ab)₂ fragments may provide good possibilities for pre-embedding EM-ISH studies in ultrastructurally well-preserved cells. Thus far, the use of ultra-small gold with silver enhancement is reported after pre-embedding ISH on Triton X-100-extracted cells. Although the detection efficiency is high, the ultrastructural morphology of the cytoplasm was not optimally preserved (26,27). Moreover, the silver enlargement of gold particles includes not well-understood steps that may influence the ef-

iciency, homogeneity, and reproducibility of the obtained signals (28,29), thus, for our purpose, making it less suitable than the immunoperoxidase/DAB technique.

In conclusion, the effects of pre-treatments on ultrastructural morphology and RNA detection efficiency can be predicted from RCM images to a large extent. Sensitive detection of DAB signals enabled visualization of small changes in ISH results owing to variations in the ISH protocol. Therefore, RCM may prove to be a powerful microscopic technique for detection of low-abundance mRNAs.

With the pre-treatments analyzed, it appeared impossible to find an acceptable balance between ISH signals and preservation of ultrastructural morphology: when good signal-to-noise ratios were obtained, the ultrastructural morphology had already deteriorated. The techniques and results presented here are useful for further development of methods that lead to an acceptable balance between RNA detection efficiency and preservation of ultrastructural morphology. Subtle dissolution of the cholesterol component of membranes in fixed cells with detergents has proven essential in this respect (Macville et al., submitted for publication).

Acknowledgments

We thank L.D.C. Verschagen for excellent electron micrographs, F. Van de Rijke and J. Van der Meulen for technical instruction, and Dr H.K. Koerten and Prof Dr H.J. Tanke for useful discussion.

Literature Cited

1. Larsson LI, Hougaard DM. Optimization of non-radioactive in situ hybridization: image analysis of varying pretreatment, hybridization, and probe labelling conditions. *Histochemistry* 1990;93:347
2. Lawrence JB, Singer RH. Quantitative analysis of in situ hybridization methods for the detection of actin gene expression. *Nucleic Acids Res* 1985;13:1777
3. Dirks RW, Van de Rijke FM, Fujishita S, Van der Ploeg M, Raap AK. Methodologies for specific intron and exon RNA localization in cultured cells by haptenized and fluorochromized probes. *J Cell Sci* 1993;104:1187
4. Binder M, Tourmente S, Roth J, Renaud M, Gehring WJ. In situ hybridization at the electron microscopic level: localization of transcripts on ultrathin sections of Lowicryl K4M-embedded tissue using biotinylated probes and protein A-gold complexes. *J Cell Biol* 1986;102:1646
5. Dirks RW, Van Dorp AGM, Van Minnen J, Fransen JAM, Van der Ploeg M, Raap AK. Electron microscopic detection of RNA sequences by non-radioactive in situ hybridization in the mollusk *Lymnaea stagnalis*. *J Histochem Cytochem* 1992;40:1647
6. Le Guellec D, Trembleau A, Pechoux C, Gossard F, Morel G. Ultrastructural non-radioactive in situ hybridization of GH mRNA in rat pituitary gland: pre-embedding vs ultra-thin frozen sections vs post-embedding. *J Histochem Cytochem* 1992;40:979
7. Landegent JE, Jansen in de Wal N, Ploem JS, Van der Ploeg M. Sensitive detection of hybridocytochemical results by means of reflection-contrast microscopy. *J Histochem Cytochem* 1985;33:1241
8. Cremers AFM, Jansen in de Wal N, Wiegant J, Dirks RW, Weisbeek P, Van der Ploeg M, Landegent JE. Non-radioactive in situ hybridization. A comparison of several immunocytochemical detection systems using reflection-contrast and electron microscopy. *Histochemistry* 1987;86:609
9. Cornelese-Ten Velde I, Bonnet J, Tanke HJ, Ploem JS. Reflection-contrast microscopy. Visualization of (peroxidase-generated) diaminobenzidine

- polymer products and its underlying optical phenomena. *Histochemistry* 1988;89:141
10. Cornelese-Ten Velde I, Wiegant J, Tanke HJ, Ploem JS. Improved detection and quantification of the (immuno)peroxidase product using reflection-contrast microscopy. *Histochemistry* 1989;92:153
 11. Prins EA, Diemen-Steenvoorde R, Bonnet J, Cornelese-Ten Velde I. Reflection-contrast microscopy of ultrathin sections in immunocytochemical localization studies: a versatile technique bridging electron microscopy with light microscopy. *Histochemistry* 1993;99:417
 12. Mello MLS, Miranda SRP. Interference analysis of heat-shocked HeLa cells. *Acta Histochem (Jena)* 1992;93:249
 13. Boom R, Geelen JL, Sol CJ, Raap AK, Minnaar RP, Klaver BP, Van der Noordaa J. Establishment of a rat cell line inducible for the expression of human cytomegalovirus immediate early gene products by protein synthesis inhibition. *J Virol* 1986;58:851
 14. Akrigg A, Wilkinson GWG, Oram JD. The structure of the major immediate early gene of human cytomegalovirus strain AD169. *Virus Res* 1985;2:107
 15. Erickson JM, Rushford CL, Dorney DJ, Wilson GN, Schmickel RD. Structure and variation of human ribosomal DNA: molecular analysis of cloned fragments. *Gene* 1981;16:1
 16. Bauman JGJ, Bentvelzen P. Flow cytometric detection of ribosomal RNA in suspended cells by fluorescent in situ hybridization. *Cytometry* 1988;9:517
 17. Vreugdenhil E, Jackson JF, Bouwmeester T, Smit AB, Van Minnen J, Van Heerikhuizen H, Kloortwijk J, Joosse J. Isolation, characterization and evolutionary aspects of a cDNA clone encoding multiple neuropeptides involved in the stereotyped egg-laying behaviour of the freshwater snail *Lymnaea stagnalis*. *J Neurosci* 1988;8:4184
 18. Artvinli S. Biochemical aspects of aldehyde fixation and a new formaldehyde fixative. *Histochem J* 1975;7:435
 19. Raap AK, Van de Rijke FM, Dirks RW, Sol CJ, Boom R, Van der Ploeg M. Bicolor fluorescence in situ hybridization to intron and exon mRNA sequences. *Exp Cell Res* 1991;197:319
 20. Ploem JS. Reflection-contrast microscopy as a tool for investigation of the attachment of living cells to a glass surface. In Van Furth R, ed. *Mononuclear phagocytes in immunity, infection and pathology*. Oxford: Blackwell, 1975:405
 21. Wolber RA, Beals TF, Maassab HF. Ultrastructural localization of *Herpes simplex* virus RNA by in situ hybridization. *J Histochem Cytochem* 1989;37:97
 22. Childs GV, Yamauchi K, Unabia G. Localization and quantification of hormones, ligands, and mRNA with affinity-gold probes. *Am J Anat* 1989;185:223
 23. Singer RH, Langevin GL, Lawrence JB. Ultrastructural visualization of cytoskeletal mRNAs and their associated proteins using double-label in situ hybridization. *J Cell Biol* 1989;108:2343
 24. Silva FG, Lawrence JB, Singer RH. Progress towards ultrastructural identification of individual mRNAs in thin section: myosin heavy chain mRNA in developing myotubes. In Bullock GR, Petrusz P, eds. *Techniques in immunocytochemistry*. Vol 4. London: Academic Press, 1989:147
 25. Pomeroy ME, Lawrence JB, Singer RH, Billings-Gagliardi S. Distribution of myosin heavy chain mRNA in embryonic muscle tissue visualized by ultrastructural in situ hybridization. *Dev Biol* 1991;143:58
 26. Sibon OCM, Humbel BM, De Graaf A, Verkleij AJ, Cremers FFM. Ultrastructural localization of epidermal growth factor (EGF)-receptor in the cell nucleus using pre-embedding in situ hybridization in combination with ultra-small gold probes and silver-enhancement. *Histochemistry* 1994;101:223
 27. Huang S, Deerinck TJ, Ellisman MH, Spector DL. In vivo analysis of the stability and transport of nuclear poly(A)⁺ RNA. *J Cell Biol* 1994;126:877
 28. Burry RW, Vandre DD, Hayes DM. Silver enhancement of gold antibody probes in pre-embedding electron microscopic immunocytochemistry. *J Histochem Cytochem* 1992;40:1849
 29. Stierhof YD, Humbel BM, Schwartz H. Suitability of different silver enhancement methods applied to 1 nm colloidal gold particles: an immunoelectron microscopic study. *J Electron Microsc Tech* 1991;17:336